Chern semi-metal and QAHE in $HgCr_2Se_4$

Gang Xu, Hong-ming Weng,

Xi Dai, and Zhong Fang

Institute of Physics
Chinese Academy of Science, Beijing

Outline

1. Introduction:

   Chern insulators, Chern semi-metal

2. Spinels family:

   FM: $CuCr_2Se_4$,$CdCr_2Se_4$, $CdCr_2S_4$, $HgCr_2Se_4$,

   AF: $ZnCr_2O_4$, $CdCr_2O_4$, $HgCr_2O_4$.

3. Magnetic Monopoles, Fermi Arcs,

   and Quantized AHE

1. Introduction: Family of TIs?

2D

T-broken

QHE

QAHE

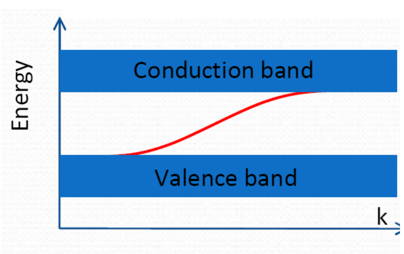

T-invariant

QSHE

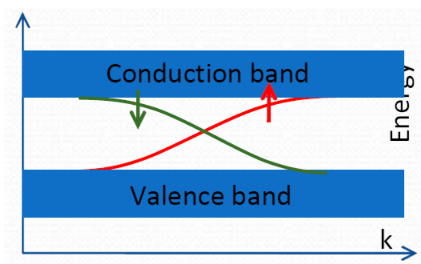

Edge States

3D

T-invariant

band

Topological Kondo Insulator

Anderson

Mott ......

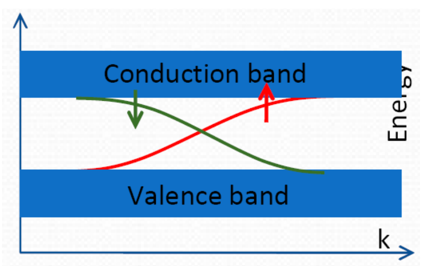

Surface States

1. Introduction: QHE vs QSHE

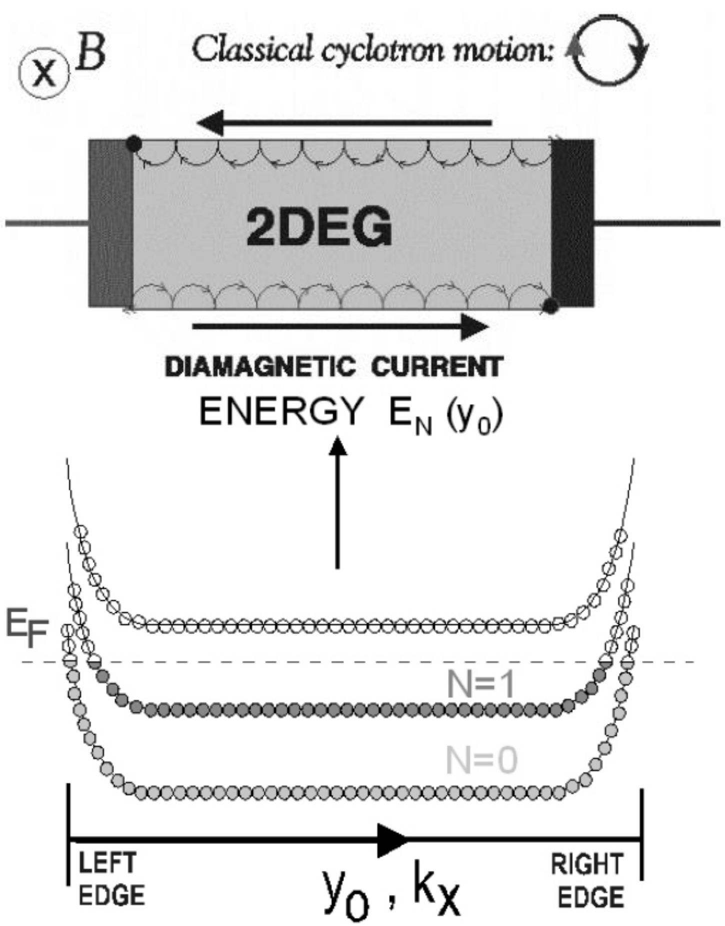

$$\Psi_{N,y_0} \propto e^{ik_x x}\cdot\Phi_N(y-y_0), \quad y_0 = \frac{\hbar k_x}{eB}$$

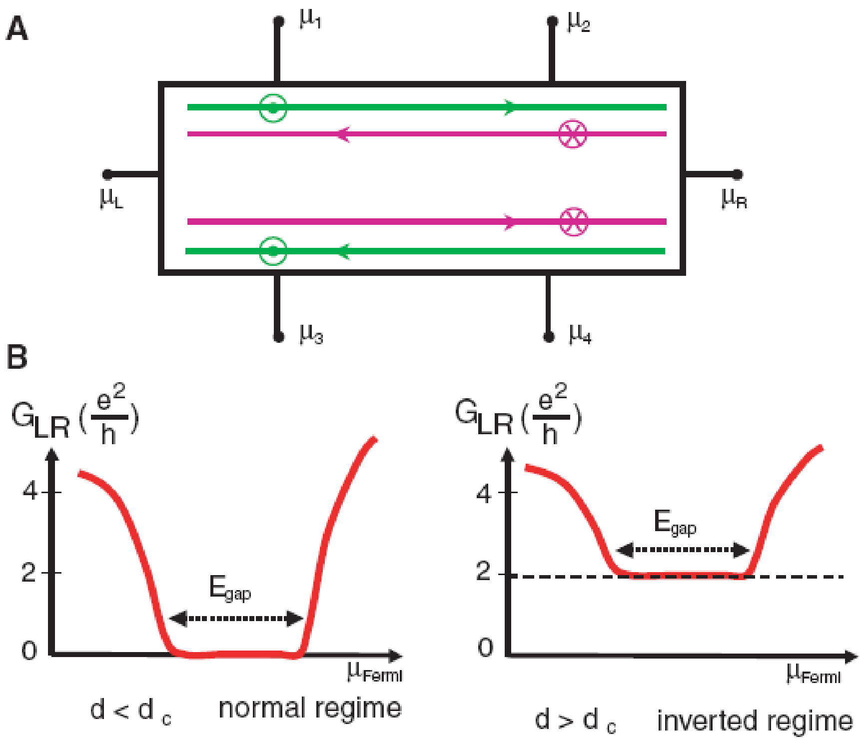

QSHE in HgTe/CdTe
(S. C. Zhang, et.al, Science 2006;
L. Molenkamp, et.al, Science 2007)

QHE
TKNN or Chern number

2D topological Insulators with TRS

1. Introduction: Chern insulators?

Broken TRS: "Quantum Hall" without external field and Landau level.

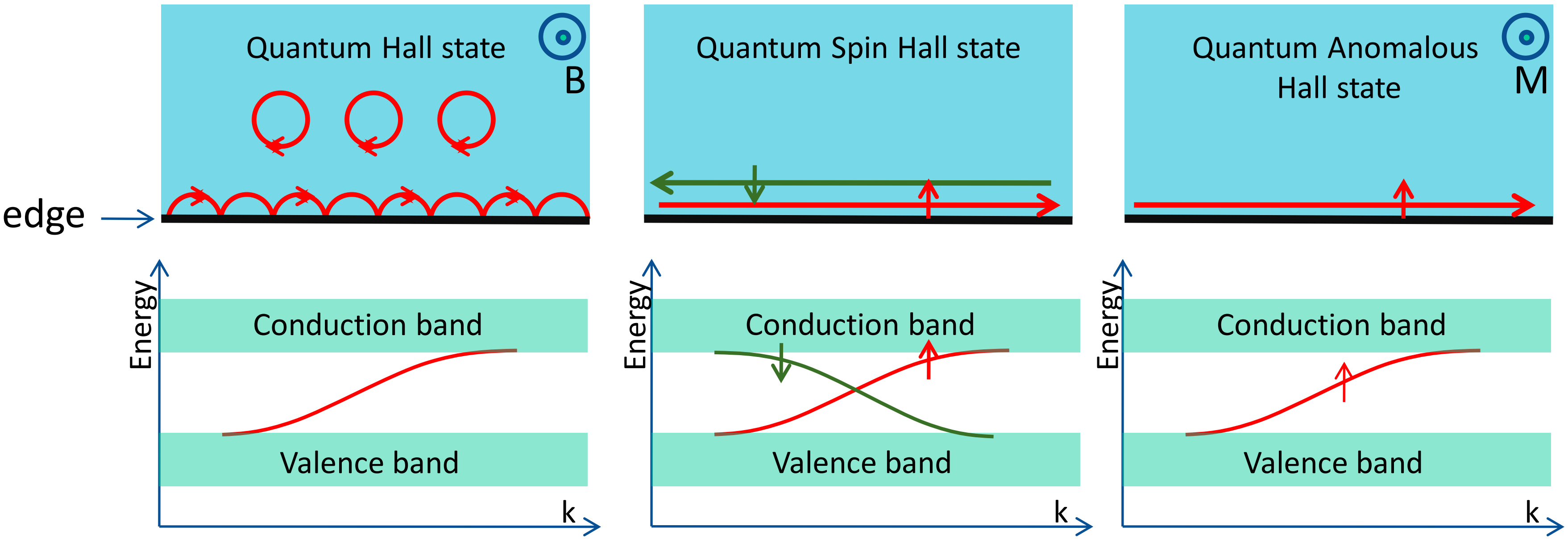

1. The QSH state can be viewed as two copies of QAH states.
2. We can destroy the TRS to keep only one of the two copies of QAH states.

1. F. D. M. Haldane, PRL (1988):

   Honeycomb lattice with staggered field (bond current).

2. Others:

   Onoda & Nagaosa (2004); localized and extended states

   Yu, Dai & Fang (2010); Magnetic topological insulatos

   A. MacDonald & Niu (2011); Graphene

1. Introduction: From 2D to 3D?

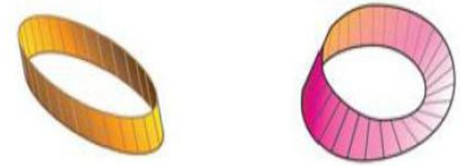

2D Topological Insulators:

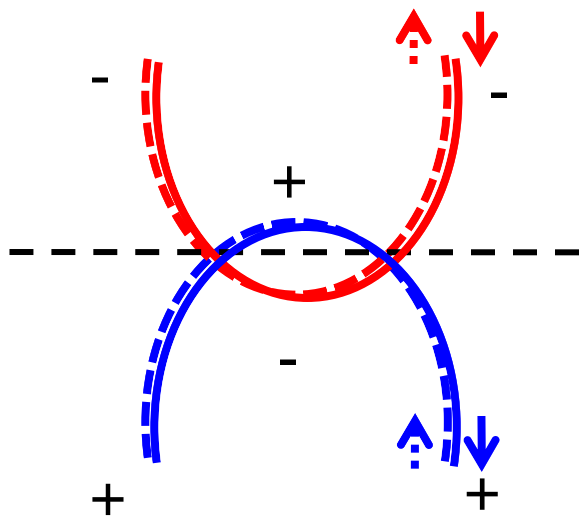

Gap opening due to SOC

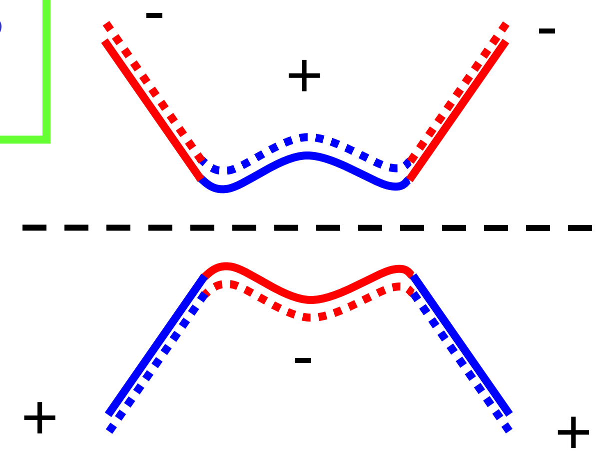

3D: (1) Weak 3D TIs:

(2) Stong 3D TIs: Time Reversal Polarization in real space!

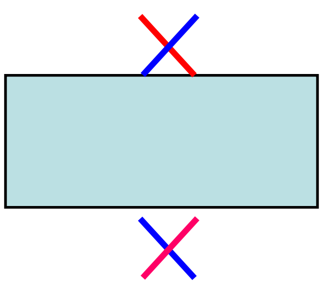

4x4 in the bulk,
2x2 on the surface
(2D Weyl nodes)

1. Introduction: From 2D to 3D without TRS?

2D Chern Insulators:

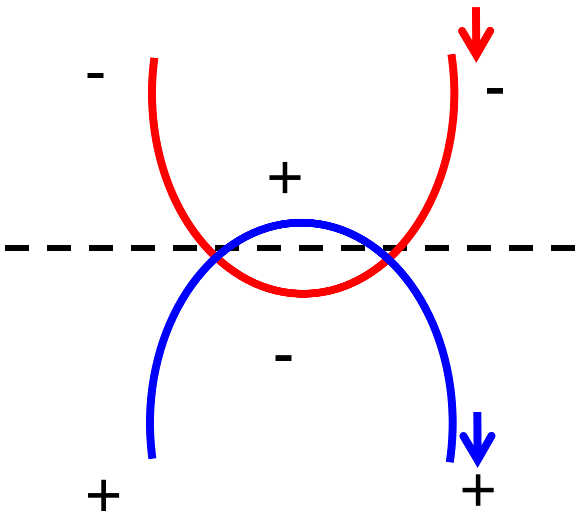

Gap opening due to SOC

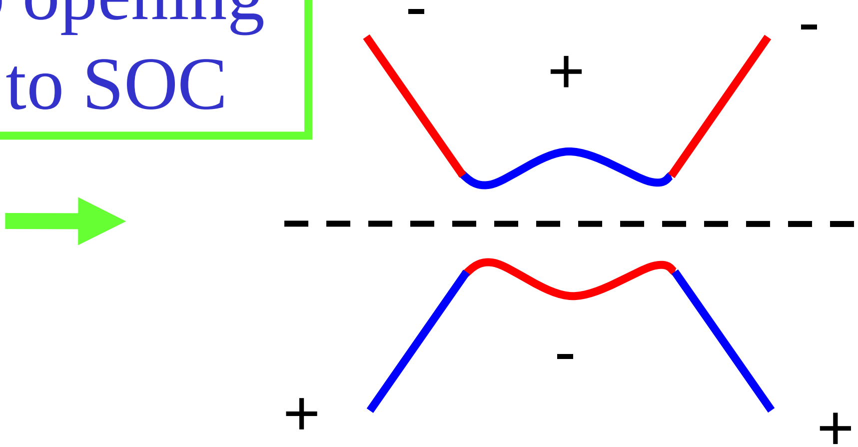

3D: (1) Weak 3D Chern Insulators:

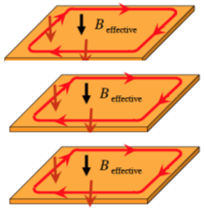

(2) Any analogy? Chern semi-metal:

Time Reversal Polarization in momentum space!

1. Introduction: Chern Insulators and semi-metal?

Weak Chern Insulators:

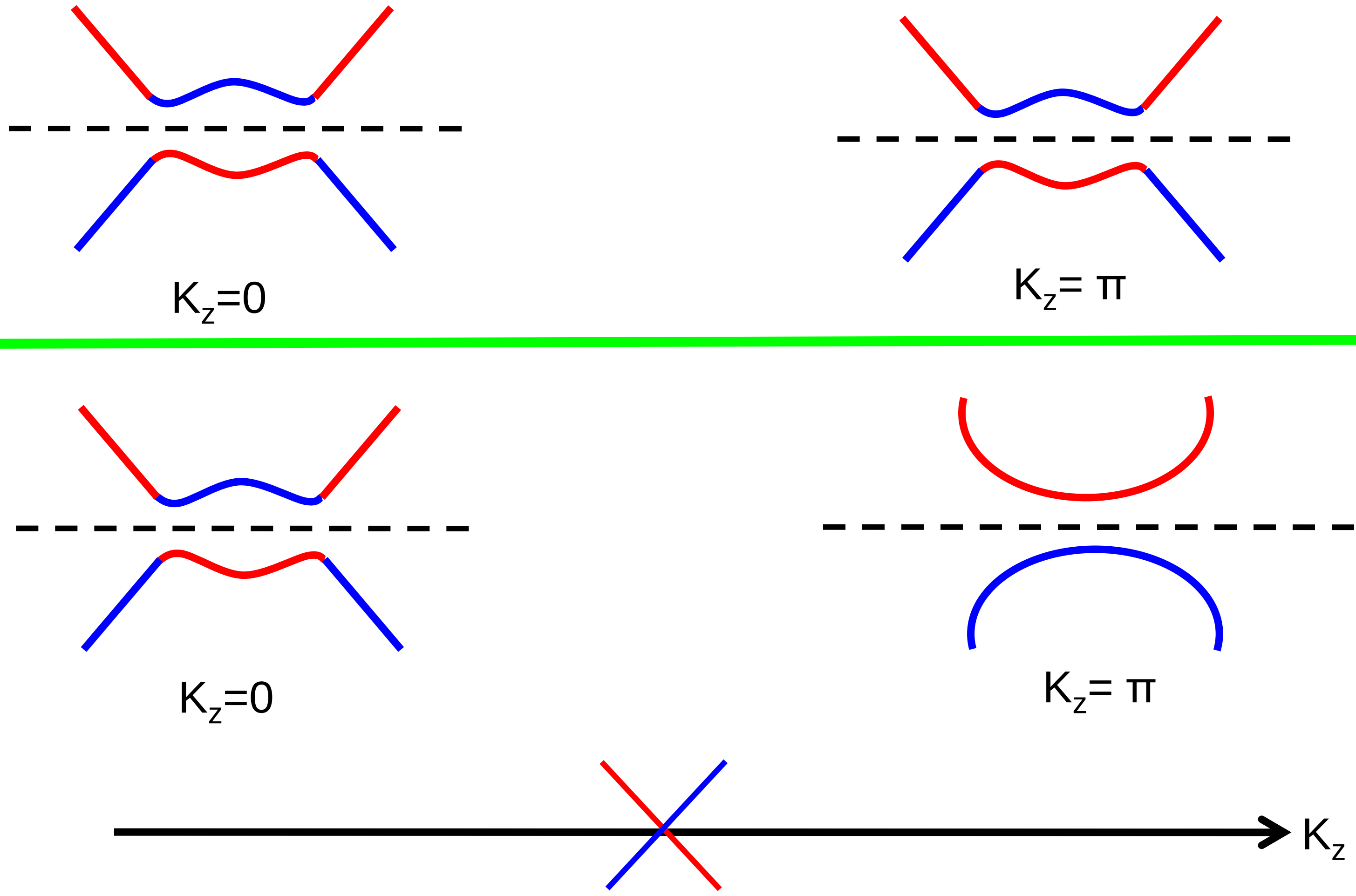

Topological Phase Transition

1. Introduction: Chern semi-metal?

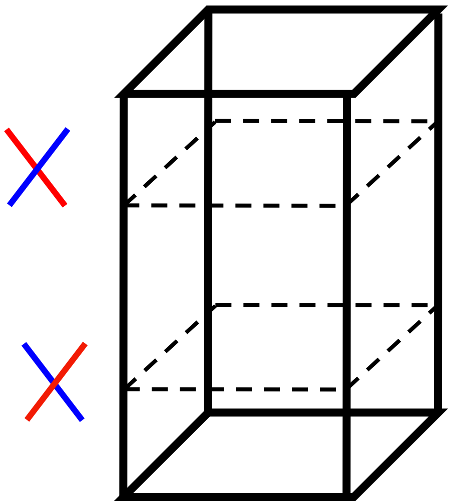

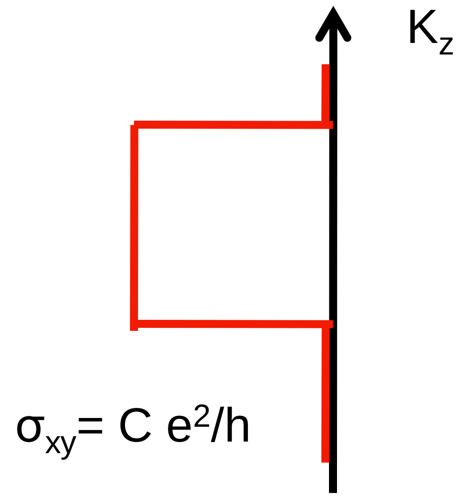

2x2 Hamiltonian in Bulk (not 4x4):

$$\varepsilon_{\pm} = \pm|\vec{f}(\vec{k})|$$

$$H(\vec{k}) = \vec{f}(\vec{k})\cdot\vec{\sigma} = \begin{bmatrix} f_z & f_x - if_y \\ f_x + if_y & -f_z \end{bmatrix}$$

Weyl nodes at: $|\vec{f}| = 0$

Berry's connection: $$\vec{A}(\vec{k}) = -i\langle u_{\vec{k}}|\nabla_{\vec{k}}|u_{\vec{k}}\rangle$$

Berry's connection: $$\vec{\Omega}(\vec{k}) = \nabla_{\vec{k}} \times \vec{A}$$

1. Introduction: Chern semi-metal?

(1) It is topologically unavoidable. (not accidental)

(2) Time-reversal polarization & Magnetic Monopoles in the K-space.

$$\vec{\Omega} = \pm \frac{\vec{f}}{|\vec{f}|^3} \quad \text{around} \quad |\vec{f}| = 0$$

(See, Z. Fang, Science (2003))

(3) Fermi arcs on the side surface.

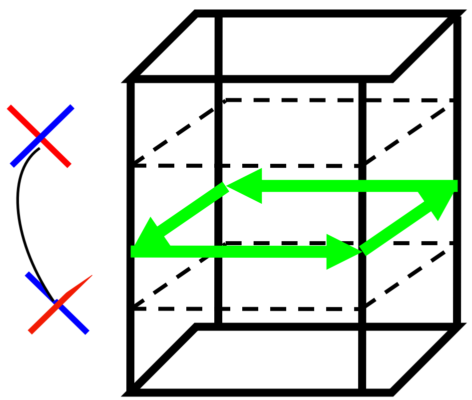

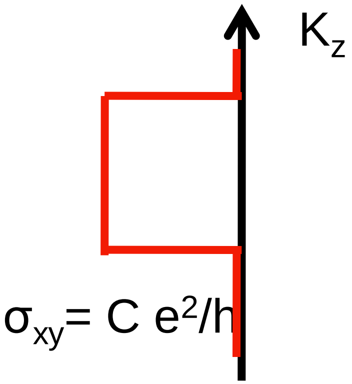

(See, X. G. Wan & Savaraso, PRB (2011), on AF Pyrochlore iridates)

(4) QAHE in quantum well structure.

Crystal structure of $HgCr_2Se_4$

Crystal structure

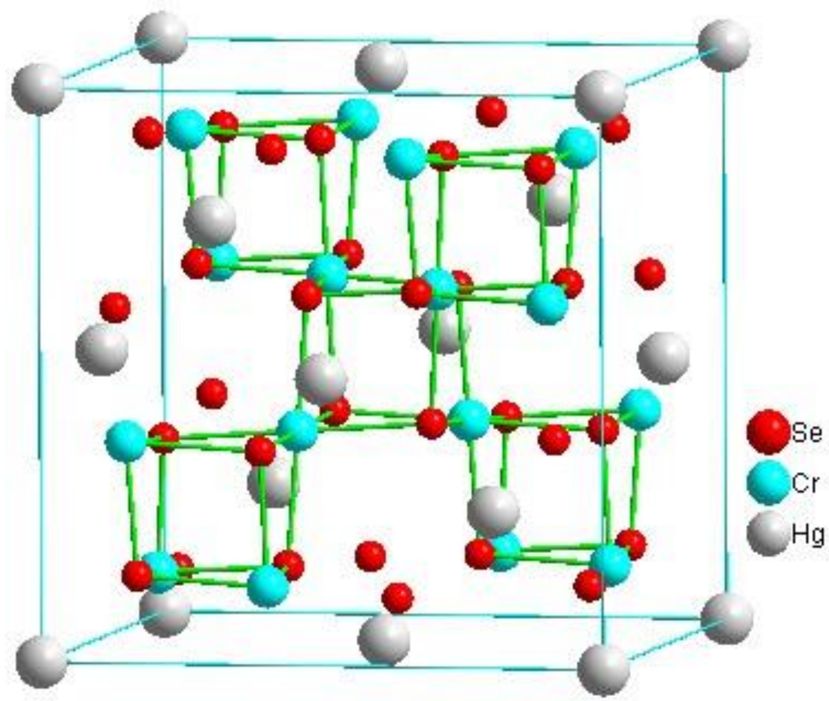

BZ

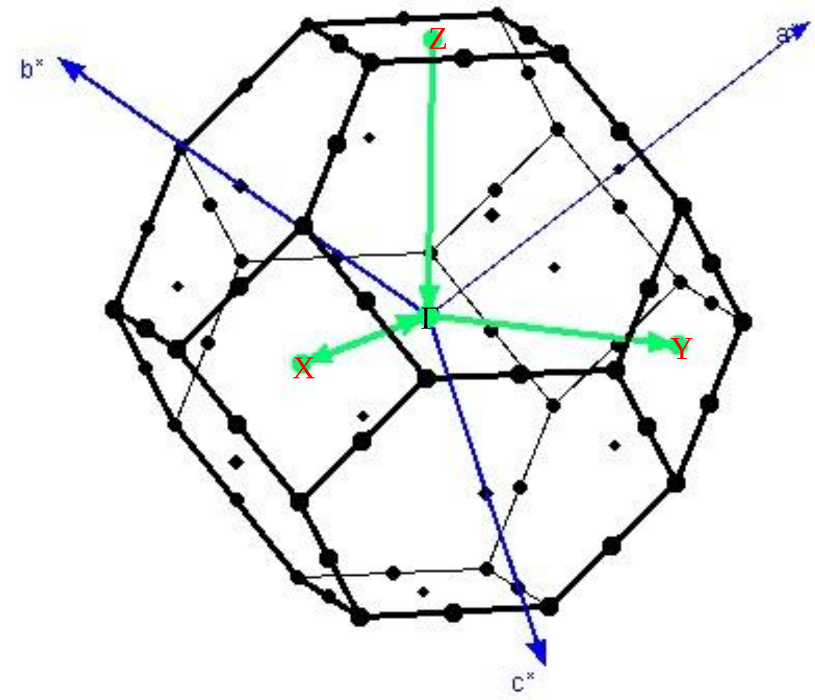

HgX sublattice is zinc-blende

Two HgX sublattice are connected by Inversion, like Diamond.

Space group Fd-3m (point group O_h).

Each Cr atom is octahedrally coordinated by 6 nearest Se atoms.

$HgCr_2Se_4$

TABLE II. Magnetic and crystallographic properties of ferromagnetic spinels.

Composition	Lattice parameter Å	u parameter	Magnetic moment (4.2°K) μ_B/molecule	Curie temp. T_c, °K	Curie-Weiss θ, °K	Curie constant C_M	θ/T_c
$CdCr_2S_4$	10.244	0.390	5.15	84.5	152	3.70	1.80
$CdCr_2Se_4$	10.755	0.390	5.62	129.5	204	3.82	1.57
$HgCr_2S_4$	10.237	0.390	5.35	36.0	142	3.62	3.94
$HgCr_2Se_4$	10.753	0.390	5.64	106	200	3.79	1.89

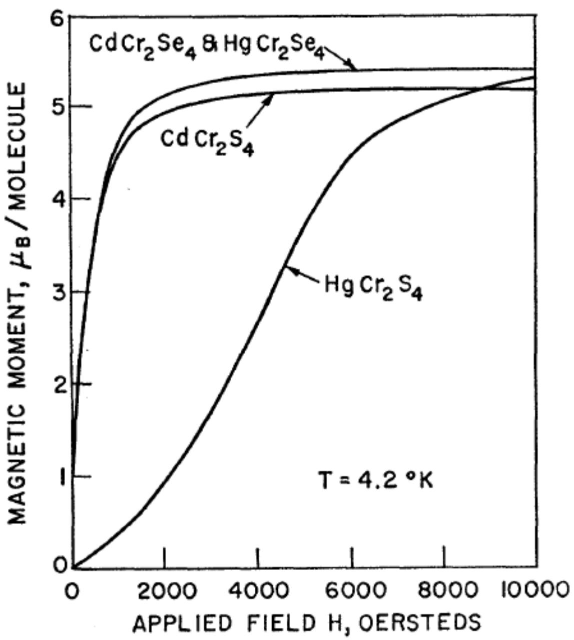

MAGNETIZATION CURVES AT 4.2° K

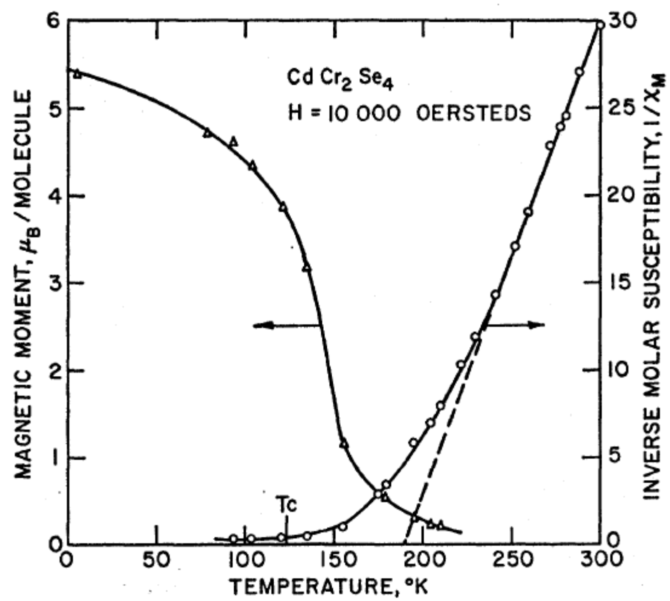

FIG. 3. Magnetic moment and inverse susceptibility as a function of temperature for $CdCr_2Se_4$ in an applied field of 10 000 Oe.

P. K. Baltzer, et.al, PRB (1966)

$HgCr_2Se_4$

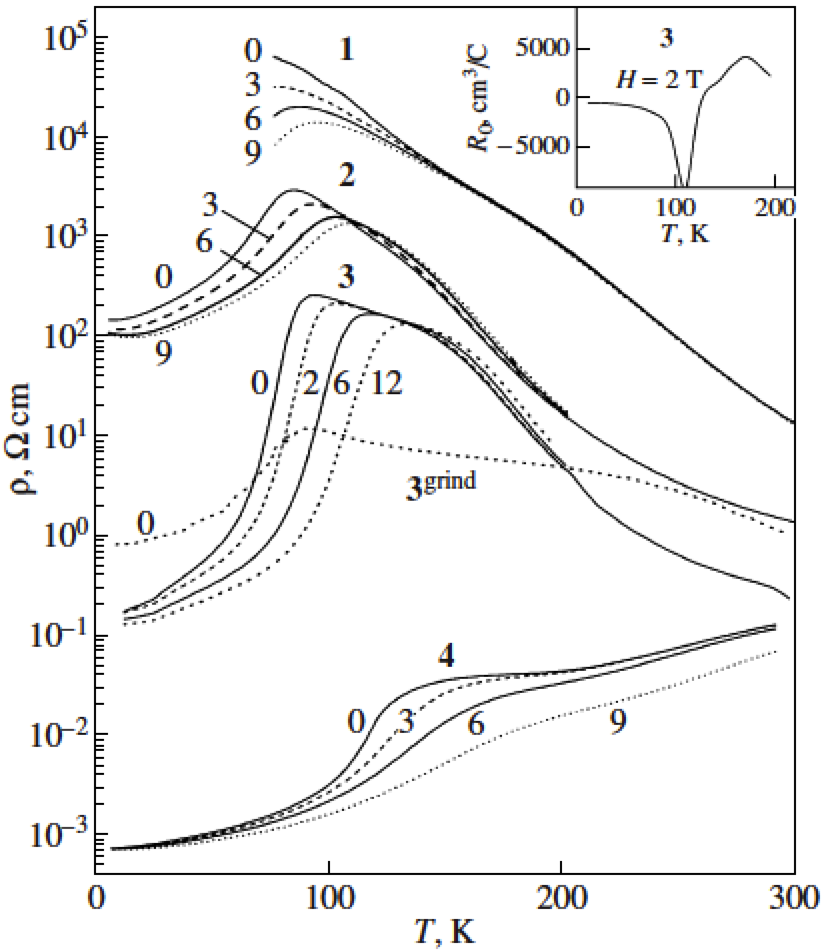

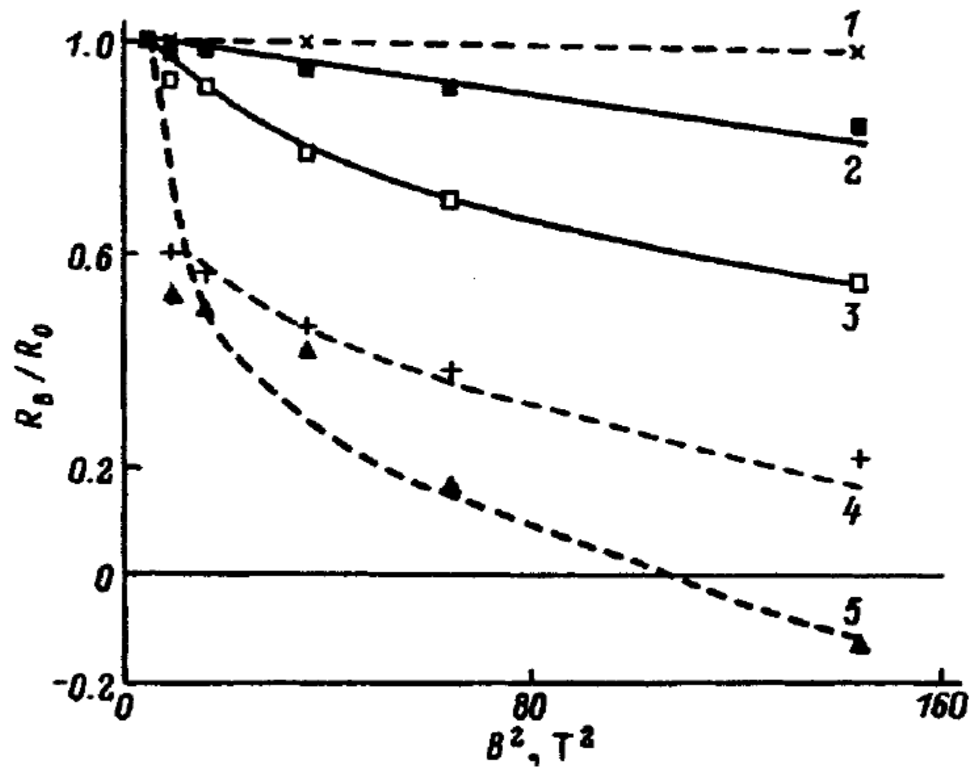

AHE
N. I . Solin, et.al,
Phys. Solid State (1996)

Metallic
N. I . Solin, et.al, PRB (2008)

Electronic structure without SOC

DOS

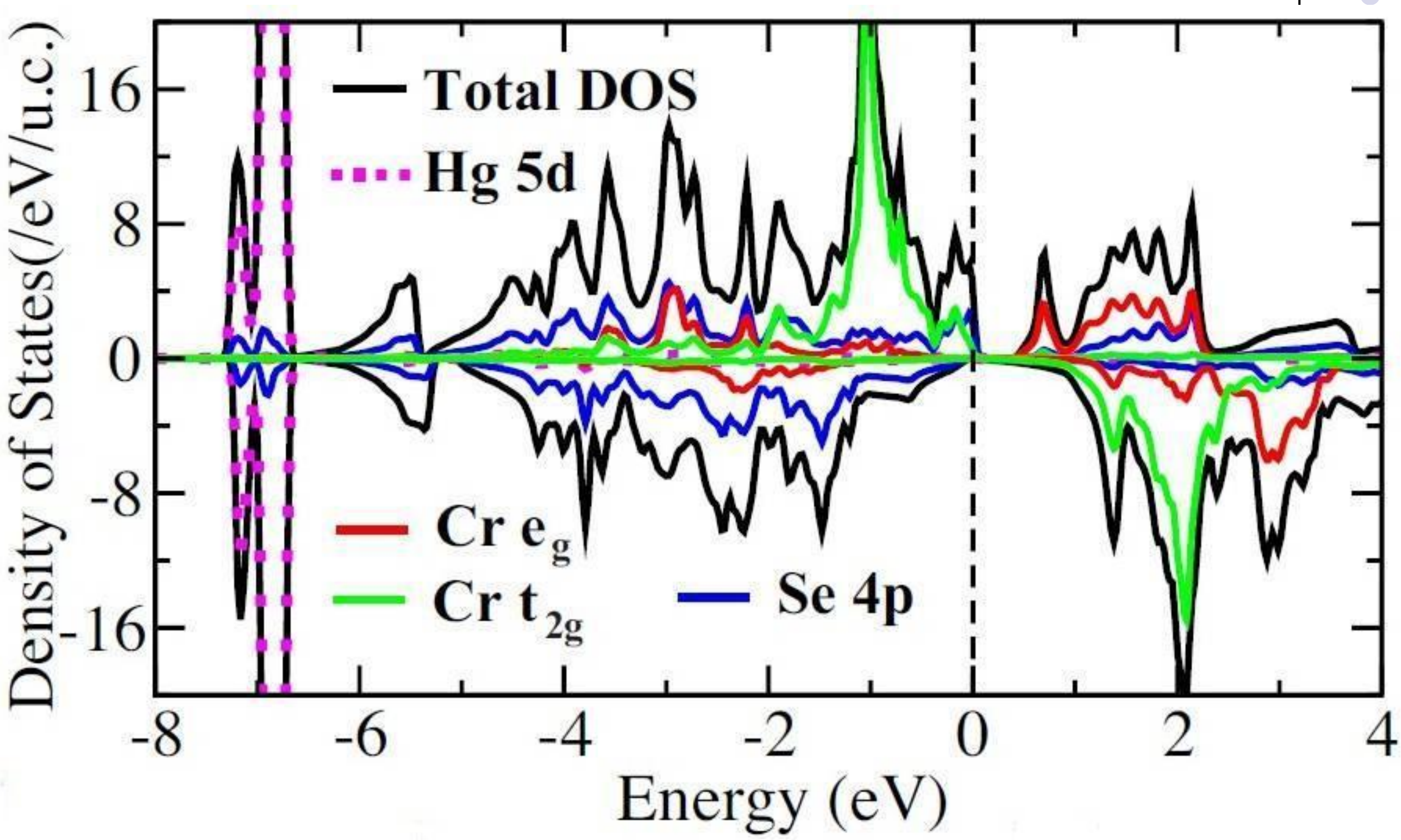

Electronic structure without SOC

Band

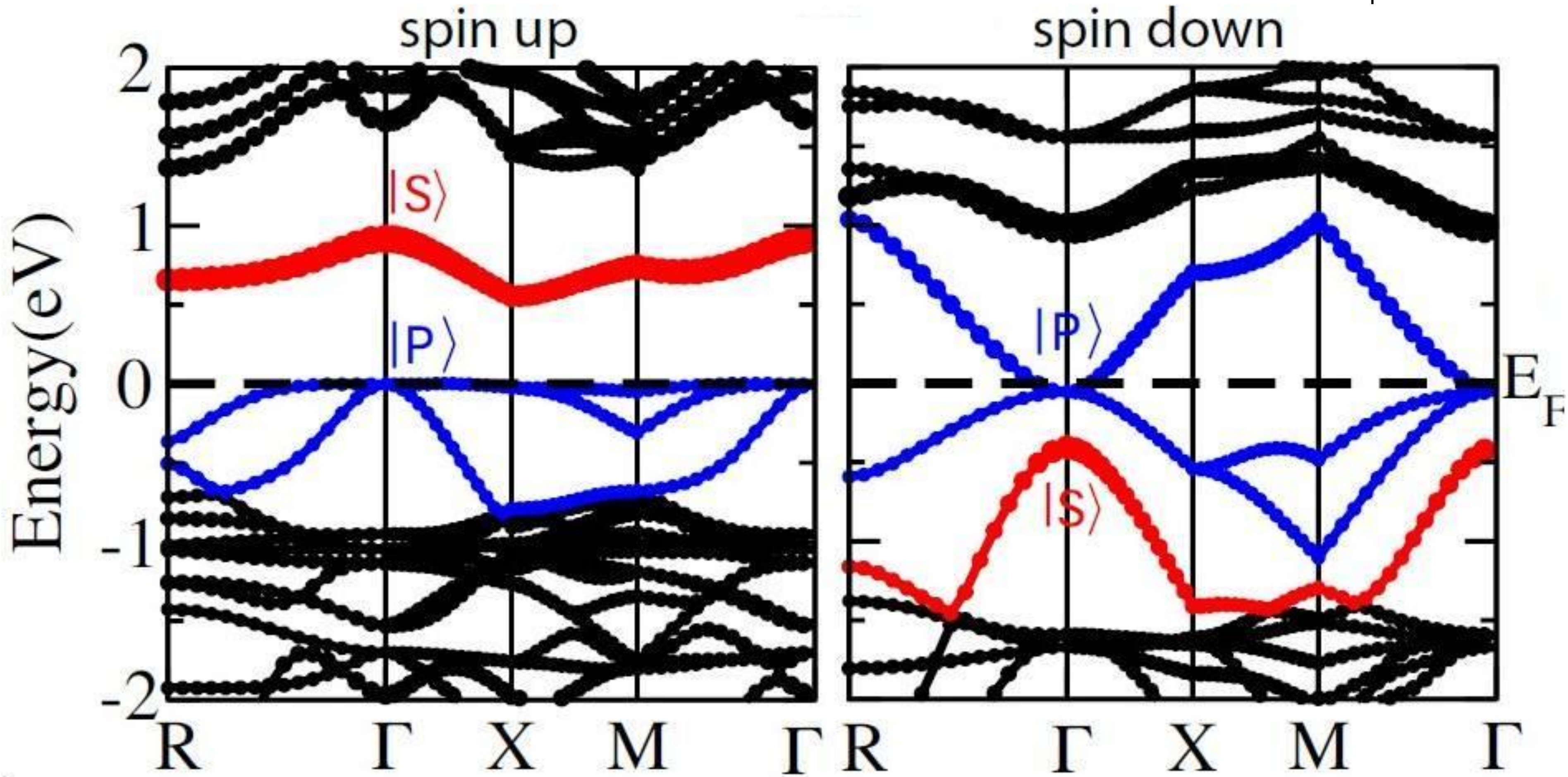

Schematic diagram for the band-inversion

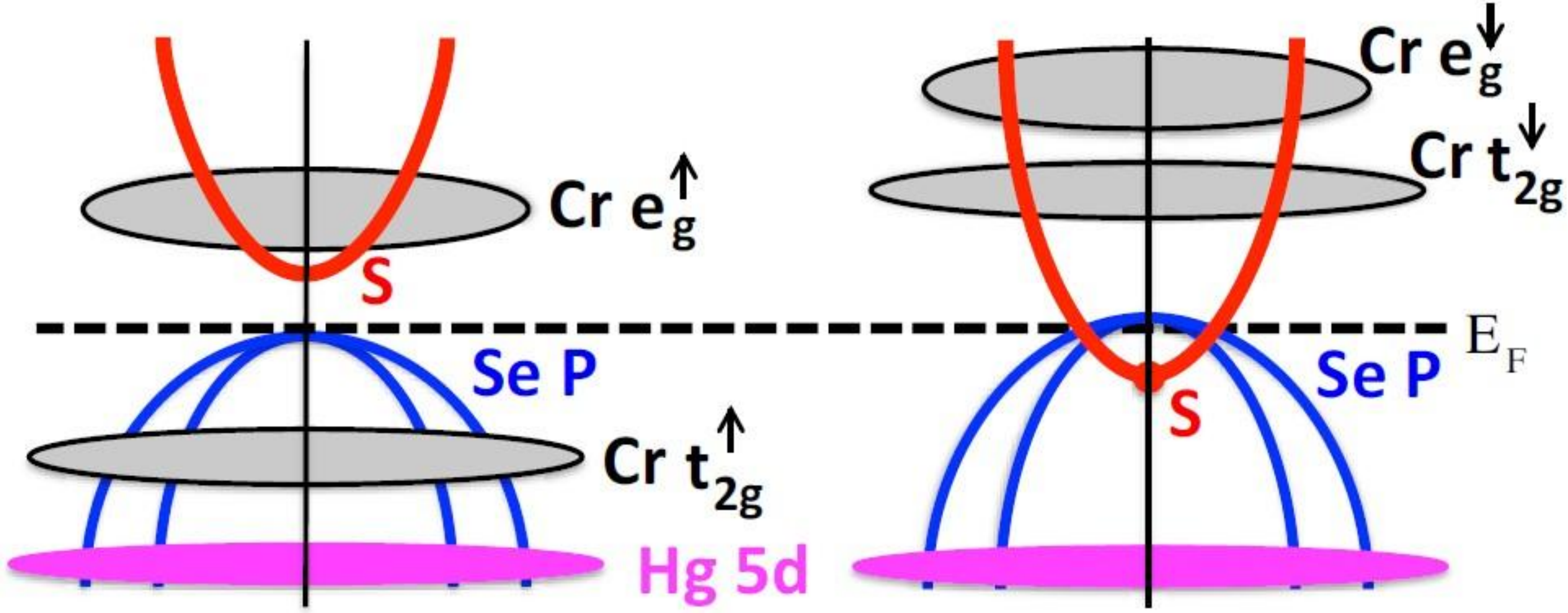

Electronic structure with SOC

low energy band with SOC

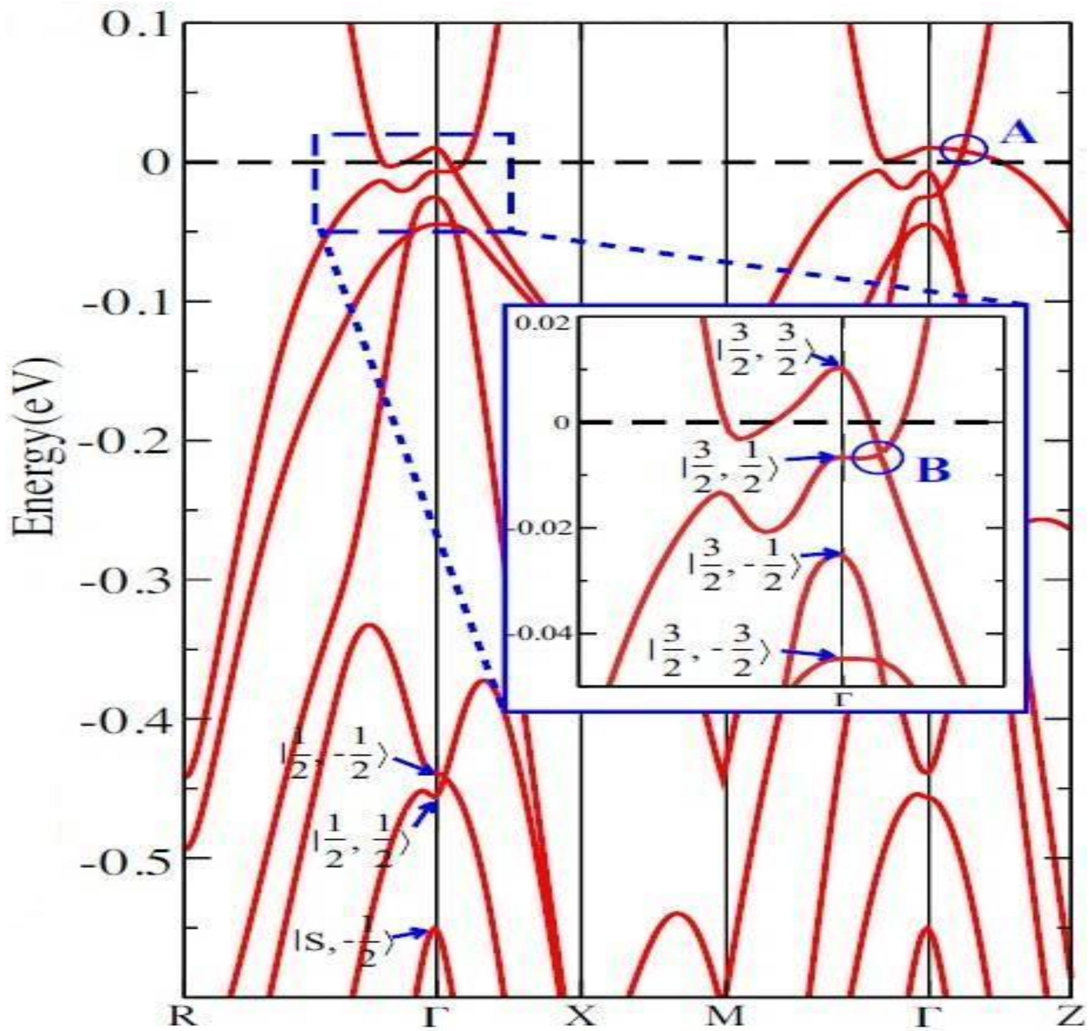

Weyl fermions and magnetic monopoles

Due to the presence of $k_{\pm}$ in the off-diagonal element, it is easy to check that Chern number C equals to 2 for the planes with $-k_z^c < k_z < k_z^c$ and $k_z \neq 0$

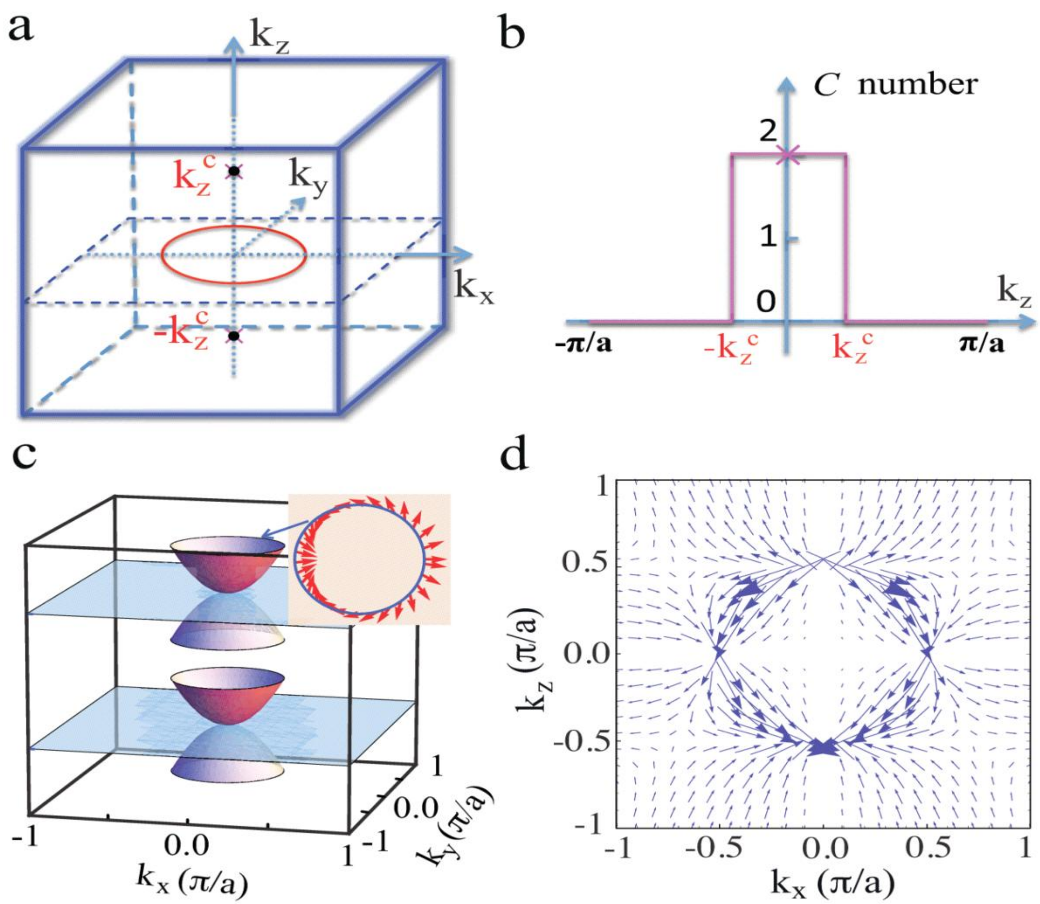

The in-plane band dispersions near the Weyl nodes $k_z = \pm k_z^c$ are thus quadratic rather than linear, with a phase of 4π for the chiral spin texture. The two Weyl nodes form a single pair of magnetic monopoles carrying gauge flux in k-space.

8-band model for HgCr2Se4

Basis

$$
\begin{aligned}
|S,\frac{1}{2}\rangle &= |S\rangle|\uparrow\rangle \\
|S,-\frac{1}{2}\rangle &= |S\rangle|\downarrow\rangle \\
|\frac{3}{2},\frac{3}{2}\rangle &= -\frac{1}{\sqrt{2}}|P_x+iP_y\rangle|\uparrow\rangle \\
|\frac{3}{2},\frac{1}{2}\rangle &= \frac{1}{\sqrt{6}}(|2P_z\rangle|\uparrow\rangle-|P_x+iP_y\rangle|\downarrow\rangle) \\
|\frac{3}{2},-\frac{1}{2}\rangle &= \frac{1}{\sqrt{6}}(|2P_z\rangle|\downarrow\rangle+|P_x-iP_y\rangle|\uparrow\rangle) \\
|\frac{3}{2},-\frac{3}{2}\rangle &= \frac{1}{\sqrt{2}}|P_x-iP_y\rangle|\downarrow\rangle \\
|\frac{1}{2},\frac{1}{2}\rangle &= -\frac{1}{\sqrt{3}}(|P_z\rangle|\uparrow\rangle+|P_x+iP_y\rangle|\downarrow\rangle) \\
|\frac{1}{2},-\frac{1}{2}\rangle &= -\frac{1}{\sqrt{3}}(-|P_z\rangle|\downarrow\rangle+|P_x-iP_y\rangle|\uparrow\rangle)
\end{aligned}
$$

Here, $|P_\alpha\rangle \approx \frac{1}{\sqrt{8}}\sum_{i=1}^{8}|p_\alpha^i\rangle$, and $|S\rangle \approx 0.4\sum_{j=1}^{2}|s^j\rangle + 0.24\sum_{k=1}^{4}|d_{t_{2g}}^k\rangle$, where $\alpha = x, y, z$, and i, j, k runs over Se, Hg, Cr atoms in the unit cell respectively. The $|s\rangle$, $|p_{\alpha=x,y,z}\rangle$, $|d_{t_{2g}=xy,yz,zx}\rangle$ are corresponding atomic orbitals of each atom.

8-band model for HgCr2Se4

Kane model without magnetic splitting

$$\begin{bmatrix}
E_s & 0 & \frac{-Rk_+}{\sqrt{2}} & \frac{\sqrt{2}Rk_z}{\sqrt{3}} & \frac{Rk_-}{\sqrt{6}} & 0 & \frac{-Rk_z}{\sqrt{3}} & \frac{-Rk_-}{\sqrt{3}} \\
0 & E_s & 0 & \frac{-Rk_+}{\sqrt{6}} & \frac{\sqrt{2}k_zR}{\sqrt{3}} & \frac{Rk_-}{\sqrt{2}} & \frac{-k_+R}{\sqrt{3}} & \frac{Rk_z}{\sqrt{3}} \\
\frac{-Rk_-}{\sqrt{2}} & 0 & E_p & 0 & 0 & 0 & 0 & 0 \\
\frac{\sqrt{2}Rk_z}{\sqrt{3}} & \frac{-Rk_-}{\sqrt{6}} & 0 & E_p & 0 & 0 & 0 & 0 \\
\frac{Rk_+}{\sqrt{6}} & \frac{\sqrt{2}Rk_z}{\sqrt{3}} & 0 & 0 & E_p & 0 & 0 & 0 \\
0 & \frac{Rk_+}{\sqrt{2}} & 0 & 0 & 0 & E_p & 0 & 0 \\
\frac{-Rk_z}{\sqrt{3}} & \frac{-Rk_-}{\sqrt{3}} & 0 & 0 & 0 & 0 & E_p-\Delta & 0 \\
\frac{-Rk_+}{\sqrt{3}} & \frac{Rk_z}{\sqrt{3}} & 0 & 0 & 0 & 0 & 0 & E_p-\Delta
\end{bmatrix}$$

where $E_s = \frac{\hbar^2k^2}{2m_s} + E_0$ and $E_p = \frac{\hbar^2k^2}{2m_p}$ with m_s and m_p being effective mass of conduction and valence bands respectively. Δ is the spin-orbit coupling energy, and $R = -\frac{i\hbar}{m_0}\langle S|\hat{p}|P\rangle$ is the momentum matrix element between conduction and valence bands.

8-band model for HgCr2Se4

Magnetic splitting term along (001) direction

$$
\begin{bmatrix}
h_s & 0 & 0 & 0 & 0 & 0 & 0 & 0 \\
0 & -h_s & 0 & 0 & 0 & 0 & 0 & 0 \\
0 & 0 & h_p & 0 & 0 & 0 & 0 & 0 \\
0 & 0 & 0 & \frac{h_p}{3} & 0 & 0 & \frac{-\sqrt{8}h_p}{3} & 0 \\
0 & 0 & 0 & 0 & -\frac{h_p}{3} & 0 & 0 & \frac{-\sqrt{8}h_p}{3} \\
0 & 0 & 0 & 0 & 0 & -h_p & 0 & 0 \\
0 & 0 & 0 & \frac{-\sqrt{8}h_p}{3} & 0 & 0 & -\frac{h_p}{3} & 0 \\
0 & 0 & 0 & 0 & \frac{-\sqrt{8}h_p}{3} & 0 & 0 & \frac{h_p}{3}
\end{bmatrix}
$$

where h_s and h_p are exchange splitting energies for the electron and valence bands respectively. By fitting from our first-principles calculations, all parameters are given as: E0 = 0.174 eV, Δ = 0.352 eV, h_s = 0.666 eV, h_p = 0.040 eV, R = $2.592 eV\,\mathring{A}$, $\frac{\hbar^2}{m_s} = 14.049 eV\,\mathring{A}^2$, $\frac{\hbar^2}{m_p} = -2.569 eV\,\mathring{A}^2$

8-band model for HgCr2Se4

Data comparing

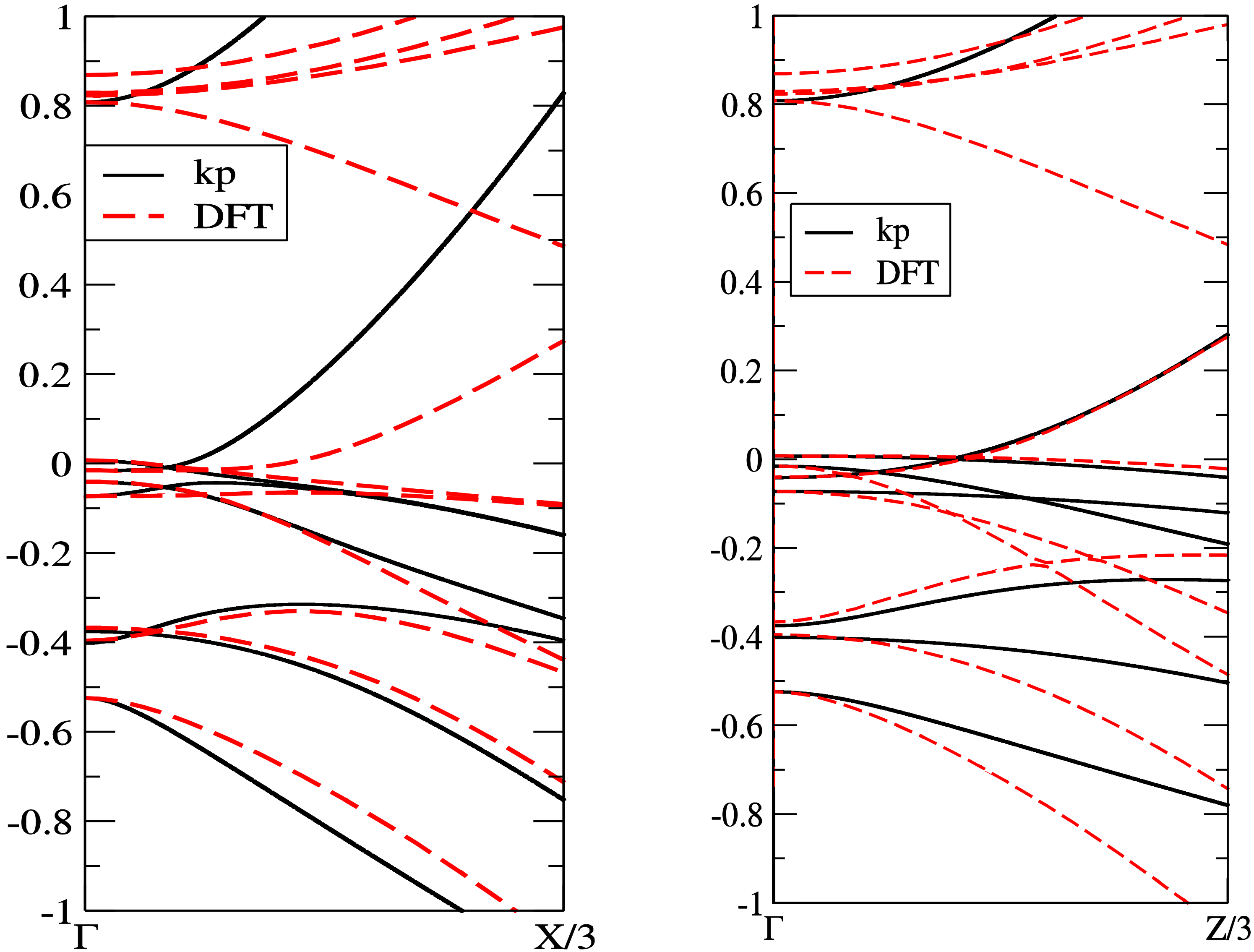

8-band model for HgCr2Se4

2-band effective model

Two basis: |3/2, 3/2> , |S, -1/2> with band-inversion

$$H_{eff} = \begin{bmatrix} M & Dk_z k_-^2 \\ Dk_z k_+^2 & -M \end{bmatrix}$$

Here $k_\pm = k_x \pm ik_y$, and $M = M_0 - \beta k^2$ is the mass term expanded to the second order, with parameters $M_0 > 0$ and $\beta > 0$ to ensure band inversion.

$$\mathrm{E}(\boldsymbol{k}) = \pm\sqrt{\boldsymbol{M}^2 + \boldsymbol{D}^2 \boldsymbol{k}_z^{\,2}(\boldsymbol{k}_x^{\,2} + \boldsymbol{k}_y^{\,2})}$$

two gapless solutions:

$$\boldsymbol{k}_z = \pm \boldsymbol{k}_z^{\,c} = \pm\sqrt{\boldsymbol{M}_0 / \beta}$$

$$\boldsymbol{k}_x^{\,2} + \boldsymbol{k}_y^{\,2} = \boldsymbol{M}_0 / \beta$$

Edge states and fermi arcs on surface

Edge state in $k_z=0.06\pi$ plane

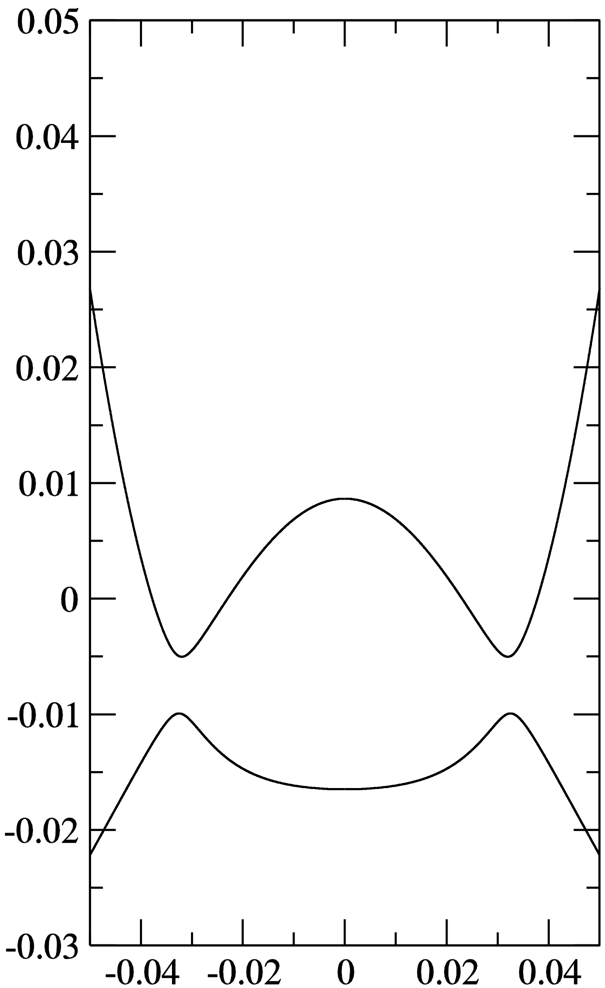

Band of bulk

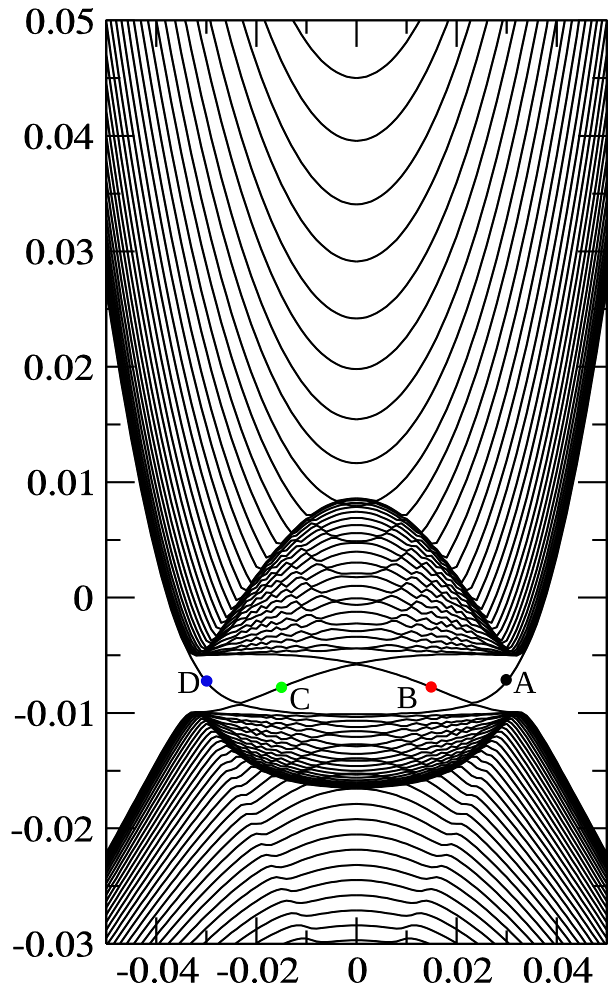

Edge state

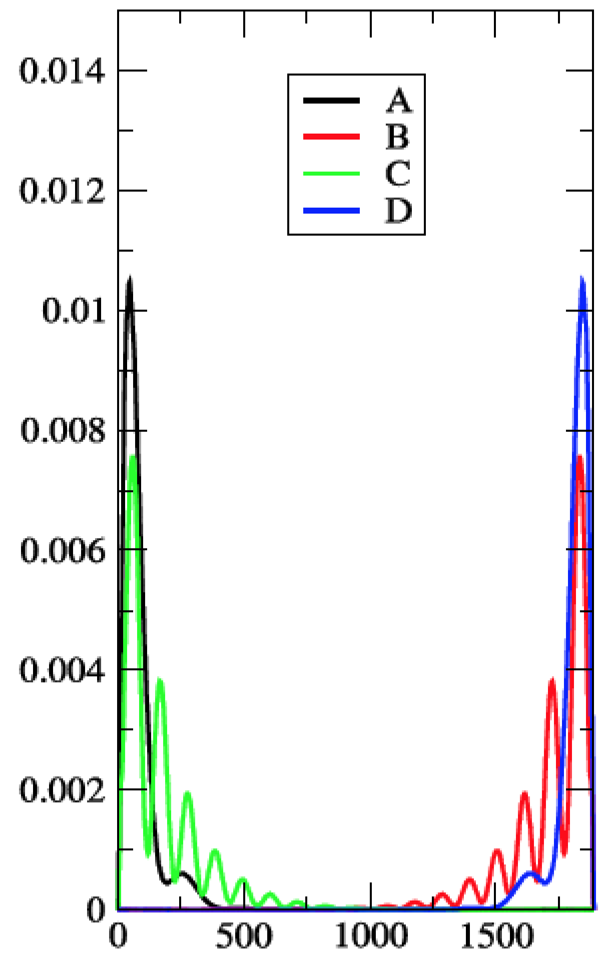

Distribution along x

Edge states and fermi arcs on surface

Edge state in $k_z=0.29\pi$ plane

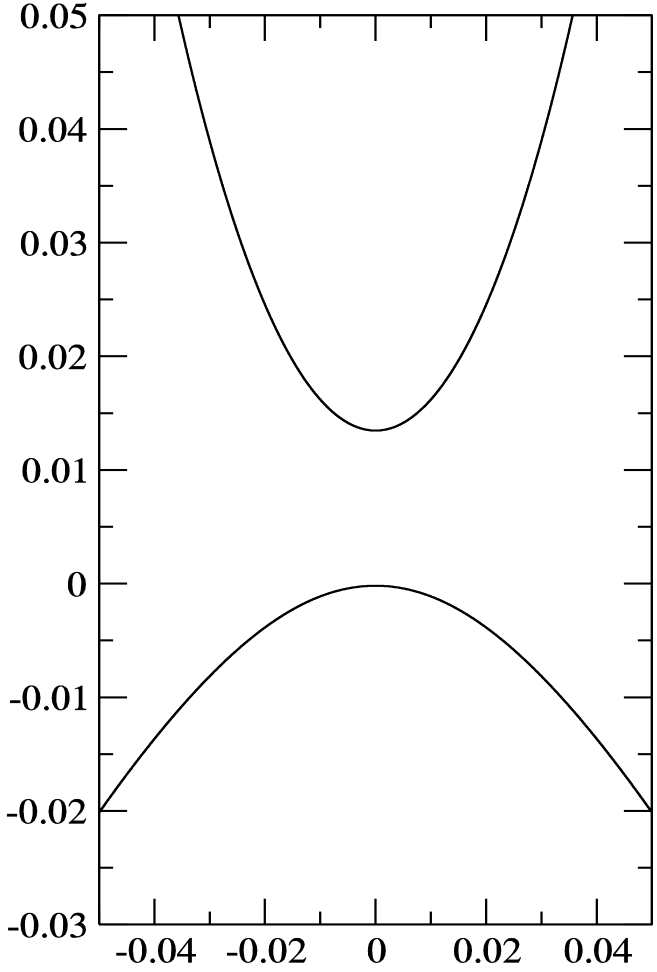

Band of bulk

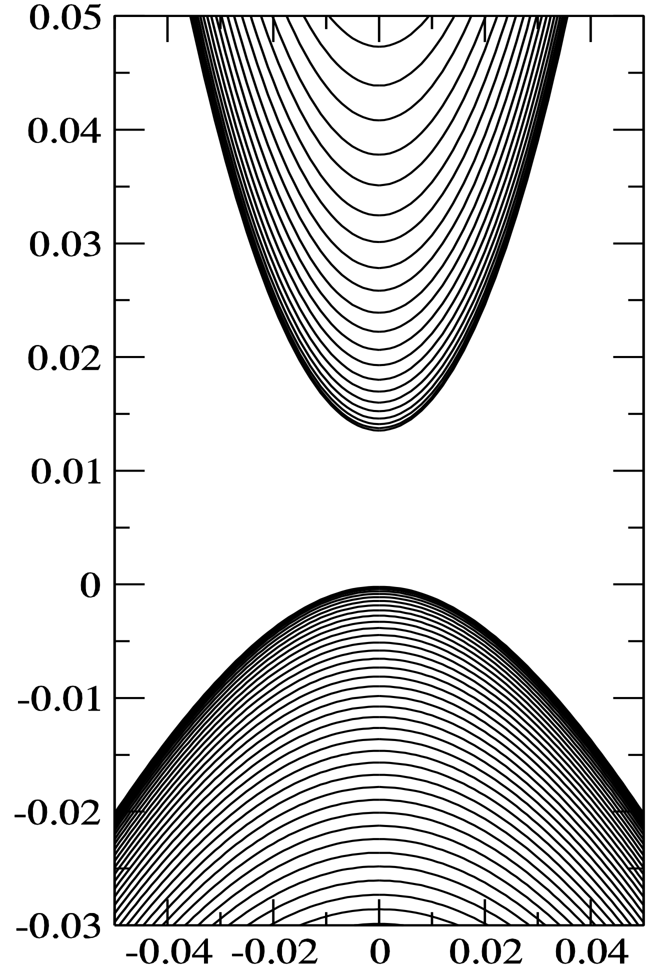

Edge state

Edge states and fermi arcs on surface

Fermi arcs for the (k_y, k_z) side surface

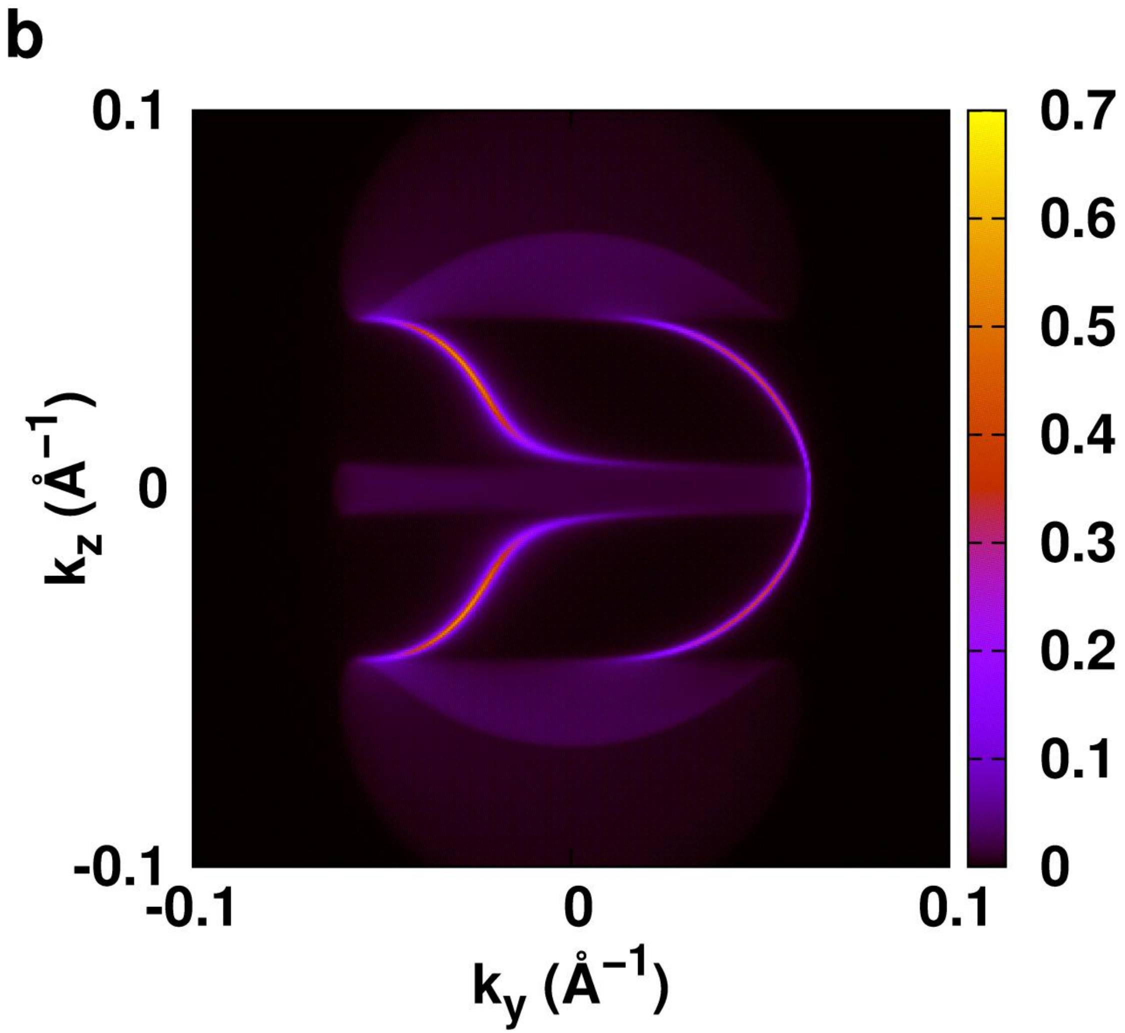

QAHE in the quantum well structure

If we consider the open boundary condition along z direction, and replace k_z by $-i\hbar\partial_z$,we can evaluate the Hall conductance in the quantum well structure.

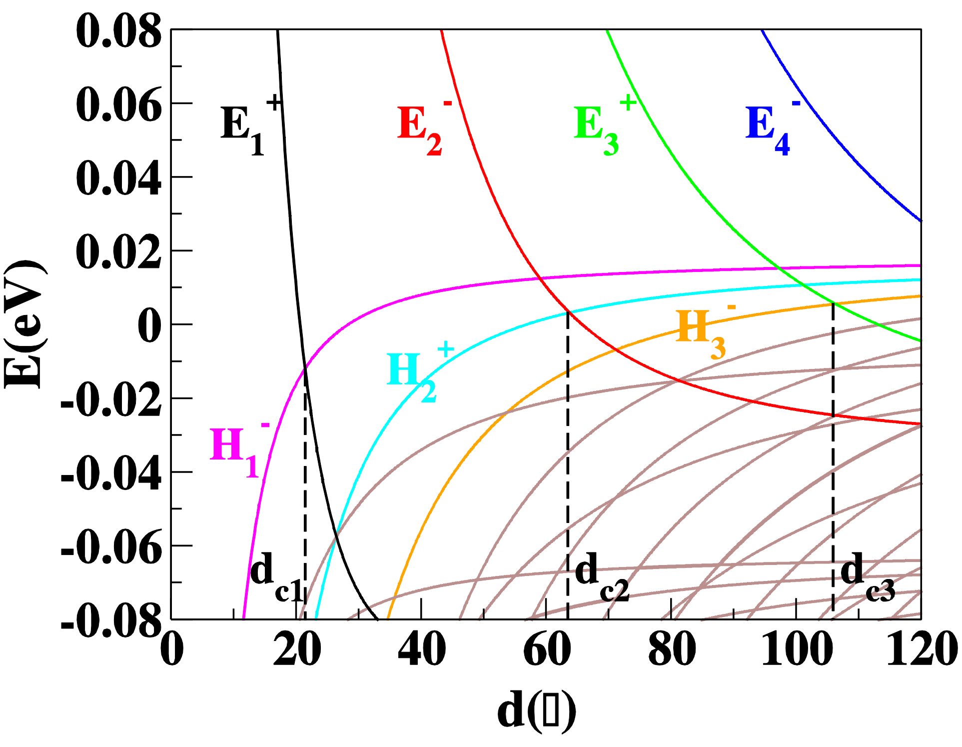

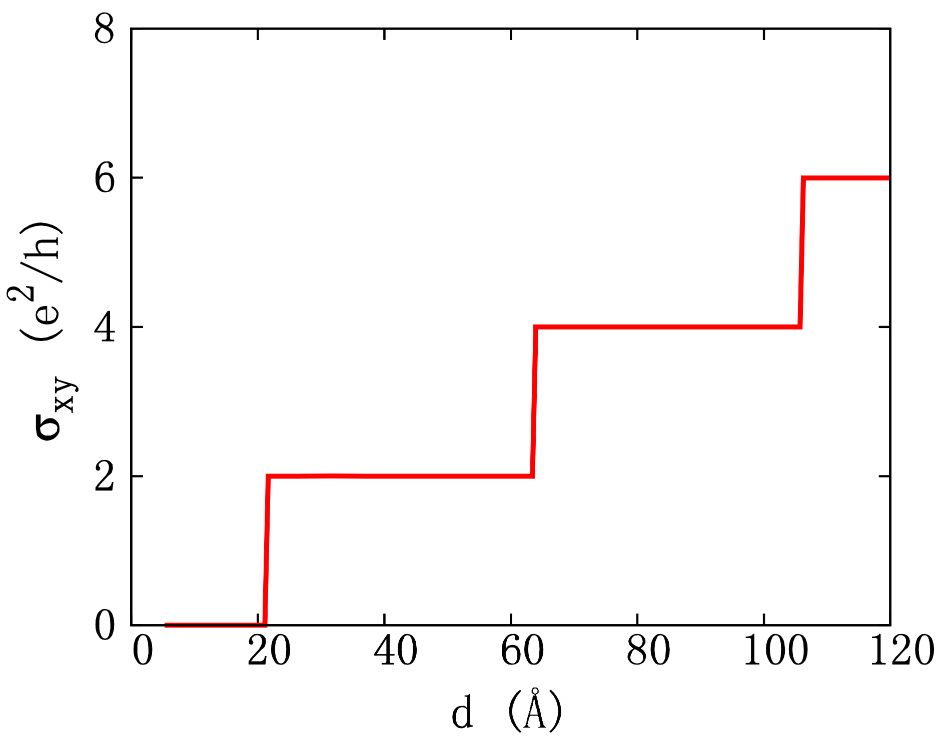

Energy gap at Γ vs. d

Hall conductance vs. d

Conclusions

✓1. $HgCr_2Se_4$ is a topological Chern semi-metal with a single pair of magnetic monopoles in the bulk.

✓2. Its Chern number shows k_z dependence from 2 to 0.

✓3. There are two fermi arcs located on each surface side, which are protected by topology.

✓4. In its quantum well structure, one can find the long-pursuing quantized anomalous Hall effect (QAHE), i.e., the quantized Hall effect without external magnetic field.

arXiv: 1106.3125 (2011)

Thank you!